Solid State Communications 250 (2017) 99–103

Contents lists available at ScienceDirect

Solid State Communications

journal homepage: www.elsevier.com/locate/ssc

Communication

Signatures of subband quantization in the Coulomb blockade regime of a disordered quantum wire

Wei Liu[a], Jianhong He[a], Huazhong Guo[a], Jie Gao[a,b,*]

[a] Department of Physics, Sichuan University, Chengdu 610064, People's Republic of China
[b] National Institute of Measurement and Testing Technology, Chengdu 610021, People's Republic of China

ARTICLE INFO

MSC:
00-01
99-00

Keywords:
A. Quantum wire
C. Boundary scattering
D. Coulomb blockade
D. Magnetoconductance enhancement

ABSTRACT

We report experiments on the two-terminal conductance of a long disordered quantum wire in a perpendicular magnetic field. Pronouncedly enhanced magnetoconductance in magnetic fields of intermediate strength is observed in the Coulomb blockade regime, which is well explained using the boundary roughness scattering and the subband quantization of the quantum wire, by modeling the disordered quantum wire as that of a quantum dot defined in a quantum wire. Assuming a parabolic constriction in the disordered quantum wire, we further obtained the magnetic field dependence of high energy levels in the quantum dot and the gate voltage dependence of the effective width of the quantum wire. Our results may provide useful information for further studies on integrated structures in on-chip laboratories.

1. Introduction

Charge transport in low-dimensional mesoscopic systems, such as quantum dots (QDs) [1–3] and quantum wires (QWs) [4–6], is of great interest for many novel physical phenomena and possible applications. Conventionally, systems like QDs usually work around the pinch off regime and are referred to as the closed systems [7], where electrons are localized and Coulomb blockade (CB) effects determine the transport properties. Whereas in open systems like QWs, the Coulomb interaction can be neglected at low energy and conductance plateaus occur [4,5]. CB effects in the QDs reflect the quantization of electron charge and conductance plateaus in the QWs reflect the quantization of subbands. The majority of work [1–6] has focused on experimental situations in which these two important effects can be cleanly separated. It seems like impossible to observe these two quantization effects in the same regime without interference [8]. However, recent theoretical studies [9–12] on disordered QWs have found a new effect of quantized subbands which may make this possible.

Due to random disorders, the interband scattering in a disordered QW is significant, leading to enormously suppressed conductance. Consequently, quantum oscillations of magnetoconductance in narrow wires are expected [9–12]. These disorders are not only defects [9] in QWs but also boundary [10,11] and interface [12] roughness. Numerical results [12] of the transport in the disordered QWs due to interface roughness, where only the two lowest subbands were populated, predicted one large magnetoconductance peak due to the depopulation of the second subband when the magnetic field B was around 2.2 T. It indicates that the second subband can participate in the transport by offering scattering states without the direct transport. Therefore, we can develop a device by connecting these QWs to a QD by weakly coupling, namely, with only one partially transmitting subband in each QW. In this case, CB effects due to the QD occur, meanwhile, the quantization of subbands is to be observed through magnetoconductance oscillations. We find that this kind of device can be easily achieved by a long disordered QW without introducing any complicated gates.

In this article, we report on a modeling and the electrical measurements of the two-terminal conductance in a disordered quantum wire. Our measurements show the enhancement of magnetoconductance in the Coulomb blockade regime due to the boundary roughness scattering and the quantization of subbands. In this case, the amplitudes of the CB peaks can be adjusted conveniently in a wide B range, which may serve as a useful tool on the integrated structures in the future. As the position of the magnetoconductance peak reflects the energy level of the subband, assuming a parabolic constriction in the disordered quantum wire, we obtain the effective width of the QW and its gate voltage dependence. Besides, our results also provide useful information of the roughness of the QW boundaries, since it is the cause of the enhancement.

* Corresponding author at: Department of Physics, Sichuan University, Chengdu 610064, People's Republic of China.
E-mail address: prof.j.gao@gmail.com (J. Gao).

http://dx.doi.org/10.1016/j.ssc.2016.08.021
Received 8 June 2016; Received in revised form 29 August 2016; Accepted 30 August 2016
Available online 31 August 2016

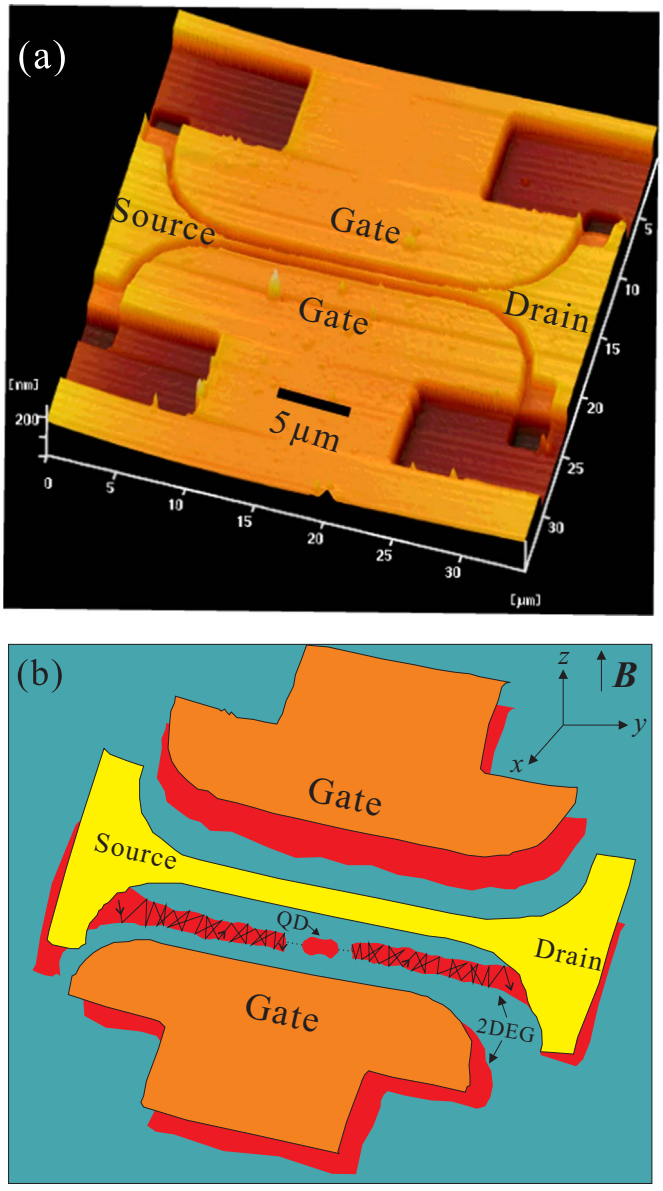

Fig. 1. (a) Atomic force microscopy image of the device. (b) Schematic picture of the device, showing the pathes of electrons in the quantum wire. Electrons travel diffusively in the quantum wire due to the boundary roughness scattering.

2. Device fabrication and layout

The materials used in our study are modulation-doped GaAs/$Al_{0.3}Ga_{0.7}As$ heterostructures prepared by molecular-beam epitaxy. A two dimensional electron gas (2DEG) situated approximately 80 nm below the surface of the devices has a carrier density of 3.0×10^{11} cm^{-2} and a mobility of 1.8×10^5 cm^2/Vs. The corresponding Fermi energy is 11 meV and the electron mean free path of the 2DEG is approximately 4.6 μm. Optical lithography was used to pattern an etch mask which protected the underlying AlGaAs from a subsequent wet chemical etch of the A1GaAs layer. Due to the interference effects during optical exposure of the photoresist, ragged edges at the base of the mask were generated, which resulted in rather rough boundaries of the wire. Then the wet chemical etch was conducted, which removed the doped layer, stopped in the AlGaAs spacer layer about 50 nm below the surface. The QW is defined by two 500 nm wide and 16.8 μm long shallow-etched trenches. Fig. 1(a) shows an atomic force microscopy (AFM) image of the device. The left and right terminals of the wire are contacted with Au/Ge/Ni alloyed Ohmic contacts, serving as the source electrode and drain electrode of the circuit respectively. The 2DEG regions on both sides of the QW serve as the side gates, as shown in Fig. 1(b). A QD is defined in the QW by impurities and its weak coupling to the QW is indicated by two dashed lines. Electrons travel diffusively in the QW due to the boundary roughness scattering. Measurements were performed in a dilution refrigerator at a base temperature of $T_{MC} = 0.3$ K and in perpendicular magnetic fields between B=0 and 5 T.

3. Results and discussions

Disorders are quite common in long QWs and they can delimit a conductance-limiting segment, referring to as the QD. Former experiments [13] in our group where similar devices were used confirmed this by measuring the characteristic “diamondlike” structures of conductance, typical effects of Coulomb blockade in closed QDs. Here we identify its existence differently by comparing the data with the typical Coulomb blockade theory. Equivalent circuit of the QW and gates are given in Fig. 2(b). In the classical Coulomb blockade regime, an approximate equation for the conductance in our experimental conditions is achieved from one former theory [1]

$$G/G_{max} \approx \sum_{N=N_0+1}^{N_0+5} \cosh^{-2}\left(\frac{(N-1/2)e^2/C - e\alpha V_g + \bar{\mu} - E_F}{2.5k_B T_e}\right) \quad (1)$$

Here, N is the number of electrons in the QD where there are already N_0 electrons before the opening of the QW, five extra electrons are added with the increase of gate voltage, e represents the electron charge, C is the total capacitance of the QD. The linear dependence of the static potential of the QD on the gate voltage V_g is given by $-e\alpha V_g$, where α defines the efficiency of gate voltage on aligning the potential. $\bar{\mu}$ is the chemical potential of the dot in equilibrium and E_F is the Fermi energy in the reservoirs. For simplicity, we assume that $\bar{\mu} \approx E_F$. k_B is the Boltzmann constant and T_e is the effective electronic temperature. The peak height G_{max} was given by [1]

$$G_{max} = \frac{e^2\rho}{2}\frac{\Gamma^l\Gamma^r}{\Gamma^l + \Gamma^r} \quad (2)$$

Here ρ is the density of states in the quantum dot. We use $\rho = \beta/\Delta E$, where ΔE is the level spacing in the QD and β is a dimensionless parameter needed to be decided in the fitting process. Γ^l and Γ^r denote the tunnel rates from energy levels in the QD to the left and right QWs, respectively. For simplicity, we assume that in our device $\Gamma^l = \Gamma^r$. The line width function $\Gamma = \Gamma^l + \Gamma^r$ and $h\Gamma$ denotes the energy level width in the quantum dot (h is the Planck constant). Normally the energy level width varies on the typical scale $h\Gamma = T\Delta E$, where T is the transmission probability of the QW. The gate voltage dependence of the transmission probability can be well described by the two-parameter Fermi distribution [14]

$$T(V_g) = \frac{1}{1 + \exp(-\frac{V_g - V_0}{\delta V})} \quad (3)$$

Here, δV decides the width on which the transmission goes from 0 to 1 and V_0 determines the gate voltage for which the transmission equals 0.5. As shown in Fig. 2(a), good agreement between experiment and theory is obtained using physically reasonable parameter values. The effective electronic temperature T_e in the device is much higher than the base temperature T_{MC}, which is acceptable taking into account the finite residual electron temperature. Large series resistance $R_{QW} = 4.16\ h/e^2$ is added in order to achieve good agreement with the experimental data. The resistance results from the boundary roughness scattering in the disordered wire and we treat it as a constant here since its variation is small in this range of the gate voltage, further discussions on this effect will be given later.

According to the fitting process, the number of electrons N_0 in the QD before the opening of the QW is 45, which indicates that the newly

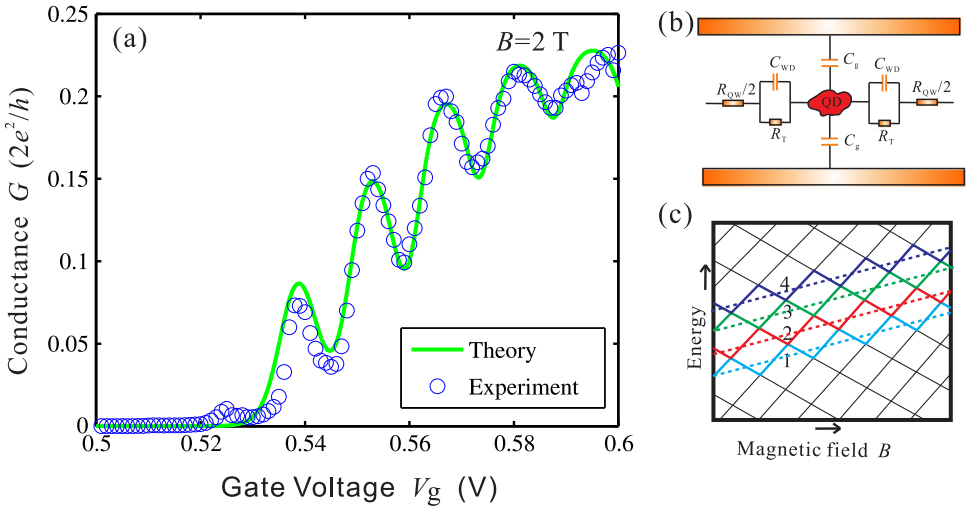

Fig. 2. (a) (Color online) Comparison between experiment (circles) and theory (trace) of the conductance in Coulomb blockade regime. Parameters of the model are $N_0 = 46$, $C = 0.0923$ fF, $\alpha = 0.1026$, $T_e = 2.08$ K, $\beta = 1.15$, $V_0 = 0.59$ V, $\delta V = 0.013$ V and $R_{QW} = 4.16$ h/e^2. (b) Equivalent circuit in which the coupling of the quantum wire and quantum dot is represented as a parallel capacitor and resistor. The coupling of the gate and dot is represented as a capacitor. The quantum wires are equalized to two resistors with the same resistance $R_{QW}/2$ for simplicity. The total capacitance C of the quantum dot is given by $C = 2C_{QW} + 2Cg$. (c) Schematic picture of the energy levels in a quantum dot as a function of magnetic field, where two Landau levels are present. Four energy levels are indicated with different colors.

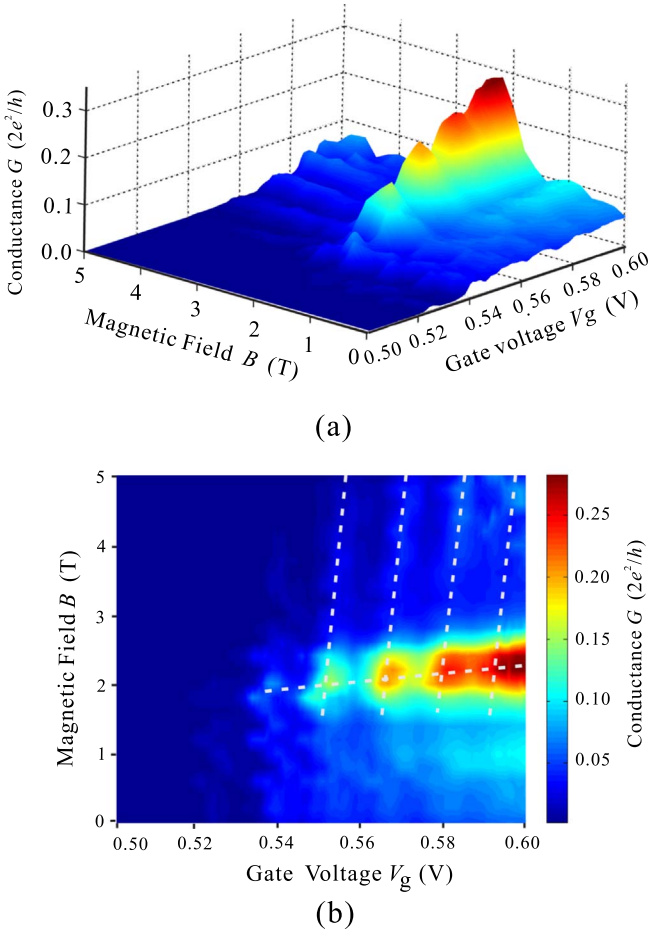

Fig. 3. (Color online) Panels (a) and (b) show the side view and top view of the color plots of the two-terminal conductance as a function of V_g and B, respectively. Four nearly vertical dashed lines indicate the positions of the Coulomb blockade peaks. The nearly horizontal dash line shows the position of the magnetoconductance peak.

added electrons with the increase of gate voltage occupy relatively high energy levels of single-particle states. In the quantum Hall regime, the energies of these states are given by the well-known Darwin–Fock states [3]. With increasing magnetic field, the energy of each state varies between different Landau levels like sawtooth with a small upward trend as indicated in Fig. 2(c). However, the sawtooth-like structures fade away very quickly with the increase of temperature, leaving only a small linear upward trend (dashed lines in Fig. 2(c)). In Fig. 3(b), four vertical dashed lines indicate the positions of the oscillation peaks in relatively stronger magnetic fields. The position of each peak changes with a small slope with the increasing magnetic field. The slope γ of the linear dependence of a single-particle state on the magnetic field can be obtained, using the relation $\gamma \Delta B = \alpha e \Delta V_g$, which gives $\gamma \approx 0.224$ meV/T. It is very small and indicates that the energies of the single-particle levels depend mainly on the gate voltage while the magnetic field only takes subsidiary function. This effect can not have a dominate impact on the coupling of the QD and the QWs, thus we can not attribute the strong enhancement of magnetoconductance to it.

Now we turn our attention to the magnetic field dependence of the transmission in the quantum wire. We consider a quantum wire formed by a parabolic constriction $m^*\omega_x^2 x^2/2$ (m^* is the effective mass of electrons in the 2DEG and ω_x is the frequency that manipulates the curvature of the potential) along the x direction and a magnetic field parallel to the z direction is applied, as shown in Fig. 1(b). The eigenenergies of the subbands in the QW are written as [12]

$$\varepsilon_n = (n + 1/2)\hbar\Omega_x + \hbar^2 k^2/2\, m^{**} \tag{4}$$

Where $n = 0, 1, 2, \ldots, \hbar$ is the Planck constant divided by 2π, $\Omega_x = \sqrt{\omega_c^2 + \omega_x^2}$, $\omega_c = eB/m^*$ and $m^{**} = m^*/[1 - (\omega_c/\Omega_x)^2]$. With the increase of B, the cyclotron frequency ω_c gets larger, leading to the subband depopulation and the increase of the effective mass m^{**}. Consequently, the density of states in each subband increases since it is proportional to $\sqrt{m^{**}}$. At low temperature, only electrons at the Fermi points (red dots in Fig. 4(b)) participate in the transport. In consequence of the rough boundaries, interband scattering among these Fermi points is significant. It is dominant when the effective mass m^{**} is large, as large densities of states (green dashed line in Fig. 4(c)) contribute to increased scattering without contributing to a significant conductivity (red solid line in Fig. 4(c)). Theoretically the boundary roughness was described by two parameters [10]: the root-mean-square deviation of the QW boundaries and its correlation length. In order to observe the boundary roughness scattering effect, both of these two parameters must be comparable to the wavelength of electrons at the Fermi energy $\lambda_F = \sqrt{2\pi/n_s} \sim 46$ nm, which is satisfied in our

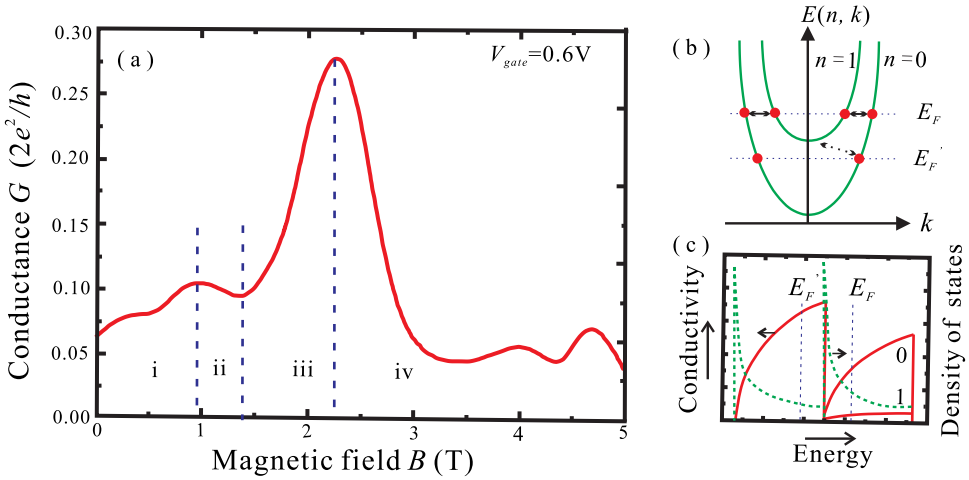

Fig. 4. (Color online) (a) Magnetic field dependence of the conductance G. See details in the text. (b) Schematic picture of the dispersion relation for the two lowest subbands indexed by $n = 0$ and $n = 1$ respectively. Two horizontal dashed lines display two positions of the Fermi energy relative to the subbands. The solid double-headed arrows demonstrate the interband scattering between the Fermi points. The dashed arrow indicates the phonon scattering. (c) Schematic picture of the conductivity and the density of states in a quantum wire as a function of the energy. Contribution to conductivity from each subband is given.

experiments by the optical lithography technique as described before.

The lithographic width of the quantum wire W is about 300 nm. However, due to the sidewall depletion effects, the effective width of the channel W_{eff} can be substantially smaller. Their difference is equal to the sum of the lateral depletion width W_{dep} at two boundaries of the QW, i.e., $2W_{dep} = W - W_{eff}$. In a former experiment [15], an etched GaAs/$Al_xGa_{1-x}As$ mesa structure of nominal width 500 nm had a effective width of 200 nm, thus giving a lateral depletion width $W_{dep} = 150$ nm. Using this value in our experiment, the wire should be depleted with a zero gate voltage, which is the actual situation in our devices. With the increase of gate voltage, the effective width slowly increases, with a rate about 0.1 μm/V [16]. When the whole system starts to conducting, the gate voltage $V_g \approx 0.52$ V, which gives $W_{eff} \approx 52$ nm. Treating the confining potential of the QW as a parabolic form, the number of occupied subbands N in the QW [17] is given by Int $[\pi W_{eff}/2\lambda_F + 1/2] = 2$. Spin splitting is suppressed though out this work due to the high electron temperature. So we only need to consider the lowest two subbands that contribute to the conductance. Therefore the QW studied here is in close analogy to the system theoretically studied in one former work [12]. Moreover, with the existence of the QD in the QW, the coupling between the QD and the second subband in the QW is very weak around the pinch off regime, and its direct contribution to conductance is very small. However, it still participates in the transport indirectly by introducing the scattering states.

Fig. 4(a) plots conductance as a function of magnetic field taken at $V_g = 0.6$ V. On increasing B, we can distinguish four regimes. With very small magnetic fields in regime I, there is a slow increase of conductance. This is followed by a small decrease in regime II. In the third regime a significant increase in conductance appears, reaching peak value which is about 4.4 times larger than that in zero magnetic field. Finally, the conductance slowly decreases at higher B in regime IV. Compared with earlier theoretical analysis [12], we get a clear understanding of these magnetoconductance regimes. The initial conductance increase can be well explained in terms of the suppression of backscattering between the Fermi points k and $-k$, since the wave functions at these states are pushed to the opposite directions by the Lorentz force [12]. With the increase of the magnetic field, the bottom of subband n=1 moves toward the Fermi energy and the scattering becomes prominent ascribed to the increasing density of states at the Fermi points, which leads to the decrease of conductance in regime II. For intermediate magnetic fields, a major enhancement appears in regime III, which is put down to the depopulation of the subband n=1, as the scattering to the Fermi points in subband n=1 disappears (see in Fig. 4(b)). In addition, the possible phonon scattering between subband n=0 and subband n=1 (shown by dashed arrow in Fig. 4(b)) becomes weaker. Applying stronger B in regime IV, the number of electrons participating the transmission slowly decreases, resulting in the decreasing conductance. Qualitatively, our results agree surprisingly well with the former numerical results [12], despite the fact that in their work they considered about the interface scattering and the fluctuations of the interface are in the growth sequence in the z direction.

Based on these explanations, the position of the magnetoconductance peak can be used to characterize the bottom of the eigenenergy of the second subband. Thus, we can further get information of the constriction in the QW using Eq. (4). Take Fig. 4(a) as an example where $B(G_{max}) = 2.2$ T, at this magnetic field the bottom of the second subband lies very close to the Fermi level, i.e., $\varepsilon(1) = (1 + 1/2)\hbar\sqrt{\omega_x^2 + \omega_c^2} \approx 11$ meV, here $\hbar\omega_c \approx 3.81$ meV. It gives us $\hbar\omega_x \approx 6.26$ meV, which characterizes the strength of the lateral confinement. We next estimate the effective width of the wire. Using the relation [17] $W_{eff} = 4\pi\hbar/m^*\omega_x\lambda_F$, we get the effective width $W_{eff} \approx 49.8$ nm, which agrees very well with earlier estimation within the experimental uncertainties. It in return provides evidence that previous qualitative analysis using subband quantization theory is reasonable. With this method we can roughly evaluate the gate voltage dependence of the effective wire width. As indicated in Fig. 3(b), a horizontal dash line shows the peak position of the magnetoconductance. When the gate voltage changes from 0.5529 V to 0.5992 V, the position of the magnetoconductance peak varies from 2.02 T to 2.279 T. Conducting similar calculations as before we get the variation of the effective wire width $\Delta W_{eff} \sim 2.06$ nm. Therefore, the rate of the effective wire width varying with gate voltage is about 45 nm/V, which is much smaller than the rate in the pinch off regime. This agrees with former experiment [18] and one explanation is that the bottom of the electrostatic constriction in the x direction varies with gate voltage. The potential is nearly parabolic when the gate voltage is in the pinch off regime, and approximates a truncated parabola with a flat bottom as the wire starts to open, resulting in a smaller rate.

Normally, well-defined Landau levels are expected when the magnetic length, $l_B = (\hbar/eB)^{1/2}$, becomes sufficiently smaller than the effective QW width. Owing to the rise of conduction band edges in the boundaries of the QW, edge states would appear and conductance plateaus would recover [4]. In our experiment, however, we do not observe any signatures of the formation of edge states – the conductance in the transport remains always much smaller than $2e^2/h$ – despite the fact that $l_B \approx 15$ nm for $B = 3$ T (nearly three times smaller than the effective width of the QW). We argue that this difference

results from the large fluctuations of the boundaries in our devices, which make the effect of boundary scattering persist to higher magnetic fields. Apart from this, an anomalous magnetoresistance peak at low magnetic field positions is expected when the boundary roughness scattering is considered [19], which is not found in our experiment neither. This can be well explained by H. Akera's theory [10], in which they found that the peak of magnetoresistance was suppressed by the localization effect in a much narrower and rougher wire. These observations again imply that the QW used in our experiment is highly disordered and interband scattering at Fermi points is dominant.

Note that the origin of the magnetic field dependence of conductance is different from one former experiment [20], where the QWs are defined by metal split gates with smooth boundaries. Unlike our experiment, increasing magnetic fields in their work decreases the scattering mainly introduced by the intentionally and unintentionally impurities, thus leads to the increase of the conductance amplitude. Besides, due to the magnetic field modification on the impurity potential, the pinch off gate voltage in their work changes significantly, which makes it difficult to considering the influence of gate voltages and magnetic fields separately. In our work, however, this effect is negligibly small as the confinement potential of the QD results from the large fluctuations of the boundaries.

4. Conclusions

In summary, we have observed the effect of subband quantization in the Coulomb blockade regime of a disorder quantum wire, where it shows up as an enhancement of the magnetoconductance. This is possible thanks to the boundary roughness scattering, which makes the higher subbands participate in the transport indirectly by offering scattering states. On increasing the magnetic field, a subband in the QW is slowly depopulated and the scattering to this subband disappears, consequently, a large magnetoconductance peak has been found. Since the position of the magnetoconductance peak characterizes the energy level of the subband, we have determined the effective width of the QW and its gate voltage dependence by assuming a parabolic constriction. Phonon scattering is significant when the thermal energy is comparable to the energy separation of the subbands [12]. Study on this part will be published somewhere else. The roughness scattering also plays an important role in other materials [11,21]. Our results may have some reference value on further experiments.

Acknowledgments

The authors thank H. Akera for useful discussion and his kind help. This research was supported by Key Program of National Natural Science Foundation of China under Grant no. 11234009.

References

[1] C.W.J. Beenakker, Phys. Rev. B 44 (1991) 1646. http://dx.doi.org/10.1103/PhysRevB.44.1646.
[2] P.L. McEuen, E.B. Foxman, U. Meirav, M.A. Kastner, Y. Meir, N.S. Wingreen, S.J. Wind, Phys. Rev. Lett. 66 (1991) 1926. http://dx.doi.org/10.1103/PhysRevLett.66.1926.
[3] L.P. Kouwenhoven, T.H. Oosterkamp, M.W.S. Danoesastro, M. Eto, D.G. Austing, T. Honda, S. Tarucha, Science 278 (1997) 1788. http://dx.doi.org/10.1126/science.278.5344.1788.
[4] J. Wróbel, T. Dietl, K. Regiński, M. Bugajski, Phys. Rev. B 58 (1998) 16252. http://dx.doi.org/10.1103/PhysRevB.58.16252.
[5] L. Worschech, F. Beuscher, A. Forchel, Appl. Phys. Lett. 75 (1999) 578. http://dx.doi.org/10.1063/1.124447.
[6] B. Weber, H. Ryu, Y.-H.M. Tan, G. Klimeck, M.Y. Simmons, Phys. Rev. Lett. 113 (2014) 246802. http://dx.doi.org/10.1103/PhysRevLett.113.246802.
[7] Y. Alhassid, Rev. Mod. Phys. 72 (2000) 895. http://dx.doi.org/10.1103/RevModPhys.72.895.
[8] S. Amasha, I.G. Rau, M. Grobis, R.M. Potok, H. Shtrikman, D.G. -Gordon, Phys. Rev. Lett. 107 (2011) 216804. http://dx.doi.org/10.1103/PhysRevLett.107.216804.
[9] J.M. Kinaret, P.A. Lee, Phys. Rev. B 43 (1991) 3847. http://dx.doi.org/10.1103/PhysRevB.43.3847.
[10] H. Akera, T. Ando, Phys. Rev. B 43 (1991) 11676. http://dx.doi.org/10.1103/PhysRevB.43.11676.
[11] H. Xu, T. Heinzel, J. Phys. Condens. Matter 24 (2012) 455303. http://dx.doi.org/10.1088/0953–8984/24/45/455303.
[12] S.K. Lyo, D. Huang, Phys. Rev. B 68 (2003) 115317. http://dx.doi.org/10.1103/PhysRevB.68.115317.
[13] W. Zhang, H.Z. Guo, H. Yuan, C.Y. Zhang, C. Lu, J. Gao, Solid. State Commun. 149 (2009) 2228. http://dx.doi.org/10.1016/j.ssc.2009.09.007.
[14] M. Büttiker, Phys. Rev. B 41 (1990) 7906. http://dx.doi.org/10.1103/PhysRevB.41.7906.
[15] K.F. Berggren, G. Roos, H. van Houten, Phys. Rev. B 37 (1988) 10118. http://dx.doi.org/10.1103/PhysRevB.37.10118.
[16] K. Gloos, P. Utko, M. Aagesen, C.B. Sørensen, J.B. Hansen, P.E. Lindelof, Phys. Rev. B 73 (2006) 125326. http://dx.doi.org/10.1103/PhysRevB.73.125326.
[17] D.K. Ferry, S.M. Goodnick, J. Bird, Transport in Nanostructures, second ed., Cambridge University Press, New York, 2009, pp. 249–255.
[18] D.A. Wharam, U. Ekenberg, M. Pepper, D.G. Hasko, H. Ahmed, J.E.F. Frost, D.A. Ritchie, D.C. Peacock, G.A.C. Jones, Phys. Rev. B 39 (1989) 6283. http://dx.doi.org/10.1103/PhysRevB.39.6283.
[19] T.J. Thornton, M.L. Roukes, A. Scherer, B.P. Van de Gaag, Phys. Rev. Lett. 63 (1989) 2128. http://dx.doi.org/10.1103/PhysRevLett.63.2128.
[20] A.A.M. Staring, H. van Houten, C.W.J. Beenakker, C.T. Foxon, Phys. Rev. B 45 (1992) 9222. http://dx.doi.org/10.1103/PhysRevB.45.9222.
[21] A.M. Gilbertson, M. Fearn, A. Kormányos, D.E. Read, C.J. Lambert, M.T. Emeny, T. Ashley, S.A. Solin, L.F. Cohen, Phys. Rev. B 83 (2011) 075304. http://dx.doi.org/10.1103/PhysRevB.83.075304.